Disjoining Pressure vs Thickness Isotherms of Thin Emulsion Films Stabilized by Proteins

Tatiana D. Dimitrova,*,[†,‡] Fernando Leal-Calderon,[†] Theodor D. Gurkov,[‡] and Bruce Campbell[§]

CNRS-Centre de Recherche Paul Pascal, Ave. Albert Schweitzer, 33600 Pessac, France, Laboratory of Chemical Physics Engineering, Faculty of Chemistry, Sofia University, 1 James Bourchier Ave., 1164 Sofia, Bulgaria, and Technology Center, Kraft Foods, Inc., 801 Waukegan Road, Glenview, Illinois 60025

In the present paper, we report measurements of the disjoining pressure vs thickness isotherms of emulsion films stabilized by proteins. A novel variant of the Mysels–Bergeron thin liquid film setup was constructed and further employed in the investigation of foam and emulsions films. The films are formed in a porous glass plate immersed in the corresponding oil phase. The disjoining pressure is directly measured by means of a pressure transducer, and the thickness is determined via light interferometry. The disjoining pressure vs thickness isotherms show different features in respect to the stabilizing protein. When the films are stabilized by bovine serum albumin (BSA) and β-lactoglobulin (BLG), a steric-like interaction comes into play being differently pronounced in the two cases. In contrast, the films stabilized with β-casein exhibit classical Derjaguin–Landau–Verwey–Overbeek (DLVO) behavior. The disjoining pressure was converted to force adopting the Derjaguin approximation, and the result is compared with force–distance laws obtained employing magnetic chaining technique (MCT); there is an excellent agreement. Similar comparison with data obtained in a surface force apparatus (SFA) experiment reveals substantial discrepancies due to the different physical state of the proteins adsorbed at a liquid–liquid and a solid interface. The experiment reported here demonstrates one important possibility for realistic modeling of the interaction between emulsion droplets.

1. Introduction

In all foam or emulsion systems, the overall stability is governed by the properties of the thin liquid films (TLF), which separate the bubbles or droplets. Pressing of two bubbles/droplets against each other under the action of different forces—e.g., surface forces, Brownian motion, gravity, etc.—leads to film formation. Much effort has been spent investigating in a controllable and reproducible way the processes of formation, thinning, and rupture of the liquid films. The first experiments in the field have been performed by the Derjaguin's group. They[1–3] designed a few setups that permit manipulation of the gas bubbles in a controllable way and pioneered the investigation of foam films. Scheludko[4] refined the construction proposed by Derjaguin and Titijevskaja[2] and introduced the capillary cell for studying foam films. In this configuration, the film is made by sucking the liquid from a biconcave meniscus. Later, Sonntag[5] invented a construction that permitted the formation of aqueous films between mercury droplets. His experiments provided the basis for studying emulsion films (i.e., liquid films formed between liquid droplets). Platikanov[6] proposed a setup for studying thin wetting films, formed between a bubble (droplet) and a solid wall. Lyklema, Scholten, and Mysels[7] elaborated the technique of forming macroscopic foam films on a glass frame. This method has undergone numerous modifications, but it remains a widely employed tool in studying foams.[8] Another convenient way to study TLF is to press a drop (bubble) to a large interface.[9,10] If the drop (bubble) is attached on a capillary,[9] then by changing the vertical position of the latter one can control the disjoining pressure in the film. To our knowledge, this experiment is the only one that provided quantitative information about disjoining pressure isotherms *of emulsion films*. Further description of all the techniques mentioned above can be found in ref 10. Currently, TLF are investigated mainly by means of the Scheludko cell, miniaturized Scheludko-type cell,[11] and Mysels cell[12,13] (described in the next section). The most important task in these studies is to simulate accurately the real conditions in the emulsion and foam systems, which means maintaining the capillary pressure and the radius of the droplets/bubbles close to their real values. The Scheludko cell seems to be a very good tool for obtaining reliable information about the surface forces acting in the particular conditions of that method. However, the technique has one important disadvantage: the capillary pressure there is very low—less than 100 Pa—while in emulsions it is much higher—

---

* To whom the correspondence should be addressed. Max-Planck-Institute for Polymer Research, Ackermannweg 10, Mainz D-55128, Mainz, Germany. E-mail: dimitrov@mpip-mainz.mpg.de.

† CNRS-Centre de Recherche Paul Pascal.

‡ Sofia University.

§ Kraft Foods, Inc.

(1) Derjaguin, B. V.; Obuchov, E. *Acta Phys. USSR* **1936**, *5*, 1.

(2) Derjaguin, B. V.; Titijevskaja, A. S. *Kolloidn. Zh.* **1953**, *15*, 416.

(3) Derjaguin, B. V.; Titijevskaja, A. S. *Discuss. Faraday Soc.* **1957**, *18* 27.

(4) Scheludko, A. *Kolloid-Z.* **1957**, *155*, 39.

(5) Sonntag, H. *J. Phys. Chem.* **1962**, *221*, 365, 373.

(6) Platikanov, D. *J. Phys. Chem.* **1964**, *68*, 3961.

(7) Lyklema, J.; Scholten P. C.; Mysels, K. J. *J. Phys. Chem.* **1965**, *69*, 116.

(8) Denkov, N. D. *Langmuir* **1999**, *15*, 3171.

(9) Binks, B. P.; Cho, W.-G.; Fletcher, P. D. I. *Langmuir* **1997**, *13*, 7180.

(10) Ivanov, I. B.; Dimitrov, D. S. In *Thin Liquid Films*; Ivanov, I. B., Ed.; Marcel Dekker: New York, 1988; Chapter 7 and references therein.

(11) Velev, O. D.; Constantinides, G. N.; Avraam, D. G.; Payatakes, A. S.; Borwankar, R. P. *J. Colloid Interface Sci.* **1995**, *175*, 68.

(12) Mysels, K.; Jones, A. *J. Phys. Chem.* **1964**, *68*, 3441.

(13) Bergeron, V. Ph.D. Thesis, University of California, Berkley, CA, 1993.

above several thousand pascals. The capillary pressure, P_c, in model systems (films with circular symmetry) can be calculated according to the formula[14]

$$P_c = \frac{2\gamma R_c}{R_c^2 - r_f^2} \quad (1)$$

where R_c denotes the radius of the capillary cell, r_f is the radius of the film, and γ is the interfacial tension. Equation 1 implies that the capillary is perfectly wetted by the liquid forming the film, which is generally the case. The capillary pressure crucially affects the rate of film thinning, governing in that way the short-time stability of the system as a whole. In a first approximation, the rate of thinning of a film (with nondeformable surfaces), V_{Re}, is related to the capillary pressure by the well-known Reynolds equation.[10]

$$V_{Re} = \frac{2h^3 P_c}{3\mu r_f^2} \quad (2)$$

where h is the film thickness and μ is the viscosity of the film phase. All the other symbols are the same as above. More sophisticated analysis of the thinning of a film of tangentially mobile surfaces under various conditions is given in ref 15.

The main goal of this study is to apply the Mysels-type cell for *emulsion* films to achieve better modeling of the real emulsion systems (which are characterized by considerably higher capillary pressures than those applied in the conventional Scheludko cell). When protein-stabilized emulsions are mimicked, there are at least three main reasons which make investigation of emulsion films (instead of foam ones) indispensable.

(i) It is well-established[16,17] that the protein adsorbs in different ways at air/water and oil/water interfaces. This can influence substantially the surface aggregation and interparticle interactions between the adsorbed moieties. As a consequence, the surface rheological properties (both dilatational and shear ones) in the two cases differ significantly.[18] This can influence film's lifetime and thinning rate.

(ii) The Hamaker constant for air bubbles interacting across an aqueous medium is about 10 times larger than the Hamaker constant for hydrocarbon layers interacting across the same water film. This can change substantially the stability of the films, especially for small thickness, where the van der Waals interactions become important.

(iii) The emulsion films provide the unique opportunity to probe the influence of the mass transfer across the interface (i.e., nonequilibrium effects) on the behavior of the studied systems. Even though this effect is not supposed to play a major role in protein-stabilized systems, it could be of considerable importance when a nonionic surfactant is present.[15] The latter is an important issue on an industrial scale of emulsion preparation, where the

(14) Toshev, B. V.; Ivanov, I. B. *Colloid Polym. Sci.* **1975**, *253*, 558.
(15) Kralchevsky, P. A.; Danov, K. D.; Denkov, N. D. In *Handbook of Surface and Colloid Chemistry*; Birdi, K. S., Ed.; CRC Press: Boca Raton, FL, 1997; Chapter 11 and references therein.
(16) Murray, B. S.; Færgemand, M.; Trotereau, M.; Ventura, A. In *Food Emulsions and Foams Interfaces, Interactions and Stability*; Dickinson, E., Rodríguez Patino, J. M., Eds.; Royal Society of Chemistry: Cambridge, U.K. 1999; p 223.
(17) Dalgleish, D. G. *Curr. Opin. Colloid Interface Sci.* **1997**, *2*, 573.
(18) (a) Graham, D. E.; Phillips, M. C. *J. Colloid Interface Sci.* **1980**, *76*, 247. (b) Benjamins, J.; Lucassen-Reynders, E. H. In *Proteins and Liquid Interfaces*; Möbius, D., Miller, R., Eds.; Elsevier Science, B. V.: Amsterdam, 1998; p 341.
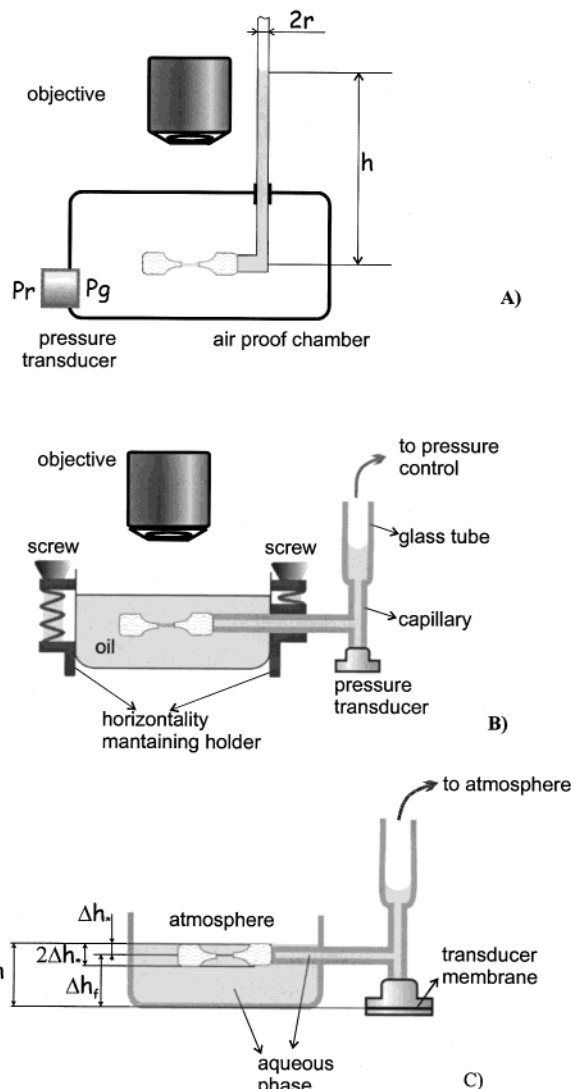

Figure 1. (a) Setup proposed by Bergeron (ref 13). The pressure jump is created by compressing the air inside the air-proof chamber. The side tube is opened to the reference atmospheric pressure. (b) The setup used in the present work in vertical cross-section. The pressure jump is achieved by sucking liquid. The big vessel is opened to the reference atmospheric pressure. (c) Pressure correction (see text for details).

nonionic surfactants are frequently added. The common nonionic surfactants are often soluble both in water and in oil, and are initially put in one of the phases. Thus, immediately after formulation of the dispersion, a process of surfactant redistribution begins. It can last for several hours, and even up to days, until equilibrium is reached. Evidently, the only way to study these processes involves emulsions films.

2. Experimental Details

2.1. Mysels-Type Cell. For foam and pseudoemulsion films Bergeron[13] (Figure 1a) has recently proposed a variant of a Mysels cell.[12] In that case, the film is formed in a hole, drilled and polished in a porous glass material. The cell is situated in an air-proof chamber. By means of a syringe pump, one creates a higher pressure of the air in the chamber, compared to the pressure of the liquid in the cell. This leads to formation of a film. The existence of highly curved menisci inside the small pores ensures much higher capillary pressure than that in the case of the conventional Scheludko cell. The maximum attainable pressure depends on the porosity and can be estimated using the simple formula $P_c^{max} = 2\gamma/r_p$, r_p being the mean radius of the pores. The

disjoining pressure in the state of equilibrium is equal to P_c. Because the pressure transducer measures only the pressure difference inside and outside the chamber,[13] one has to determine also the height, h, of the aqueous column in the capillary tube of radius r. Two corrections should be made: the first one takes into account the hydrostatic pressure in the tube, and the second one accounts for the pressure jump, which is due to the meniscus in the capillary. The final expression for the disjoining pressure reads

$$\Pi = \Delta P - \Delta\rho gh + \frac{2\gamma}{r} \tag{3}$$

where $\Delta P = P_g - P_r$, $\Delta\rho$ is the density difference (water minus air), and g is the acceleration due to gravity. The film is observed in reflected monochromatic light and different parameters, such as the film thickness, its dynamics, lifetime, etc., can be determined. It is clear that this configuration could hardly be used for emulsion films due to numerous technical difficulties. For example, to find a precise pressure transducer resistant to the organic liquids that are frequently used as oil phases (for example, xylene, styrene, hydrocarbons) is not a trivial task. On the other hand, the liquids are incompressible, hence the application of a pressure jump on the two sides of the chamber will encounter numerous practical difficulties.

We developed a new version of the Mysels-type cell that allows relatively convenient operations with both foam and emulsion films. In the setup proposed by us (Figure 1b), the film is formed in a circular porous plate by sucking liquid and the cell is directly connected to the pressure transducer (Omega PC 136 G 01 or Omega PC 136 G 05, depending on the studied pressure range), the reference pressure being the atmospheric one. The maximum attainable capillary pressure is determined as in the previous case. This configuration provides the opportunity to investigate *both* foam and emulsion films. When the construction shown in Figure 1b is used, the measured value for the pressure, P, should be corrected for the hydrostatic pressure difference between the plane of the film and the level of the measuring membrane of the transducer (see Figure 1c). That difference was obtained by calibration in the following way: the cell was filled up with the appropriate aqueous phase to the point where the upper edge of the porous plate is exactly at the level of the aqueous phase (Figure 1c). The measured pressure is

$$P = \Delta\rho g\Delta h = \Delta\rho g\Delta h_f + \Delta\rho g\Delta h_* \tag{4}$$

where $\Delta\rho$ is the density difference between water and air, and the heights Δh, Δh_f, and Δh_* are shown in Figure 1c. The value $2\Delta h_*$ can be measured directly with sufficient precision; thus, Δh_f is determined from eq 4. Let us now consider the situation when a film is formed. If in the system of Figure 1c the big vessel containing the cell is filled up with oil (aqueous emulsion films), then the real capillary pressure, P_c, is given by the following relation:

$$P_c = -P_m + \Delta\rho g\Delta h_f + \Delta\rho_1 g\Delta h_* \tag{5}$$

Here, P_m is the measured pressure, and $\Delta\rho_1$ is the density difference between oil and air. All other symbols are the same as above. Note that the lower the pressure is the higher the relative contribution of the corrections becomes. The cell is open to the atmosphere, which is very convenient from a practical point of view, especially when studying emulsion films. For foam films, the term with $\Delta\rho_1$ in eq 5 will vanish. In this case, 2 mL of the corresponding surfactant (protein) solution is placed in the bottom of the big vessel (total volume ca. 20 mL) and the latter is covered by a glass slide. This is done to saturate the vapor pressure inside the chamber, thus preventing the evaporation from the film phase.[13] The whole construction is made out of glass, which permits an easy and reliable cleaning in respect to surface active material.

Special care is taken when the transducer is fixed to the glass cell. There should be no air bubbles in the connecting glass tube. Otherwise, the measured value of the pressure will be incorrect. When the disjoining pressure is increased, the liquid in fact flows through the porous material, which is intrinsically connected

with considerable viscous drag. That is why the capillary pressure is to be increased in steps and after each increase the flow inside the porous plate has to relax before the measurements of the capillary pressure and film thickness are taken. The time necessary for the relaxation of the flow can be estimated considering the Kozeny−Carman equation for flows through porous media.[19] On average, waiting 20 min after each pressure increase is sufficient.

The cell is attached on the table of an Axioplan Zeiss microscope, employing a special homemade device, which provides a possibility to adjust the horizontality of the cell by means of two screws (Figure 1b). The horizontality is absolutely necessary to ensure that the plane of the film coincides completely with the focal plane of the objective. This is required for reliable determination of the film thickness. The microscope is equipped with long focal distance objectives (Zeiss 20×, 32×, 50×) and with a monochromatic light source. The experiments were recorded by means of a highly sensitive video camera, Sony SSC−C370P, and VCR, Panasonic AG-7335. The film thickness (effective water thickness) is determined via standard interferometry.[20] The intensity of the reflected light is connected with the film thickness via the expression

$$h = \frac{\lambda}{2\pi n_0}\left(k\pi + \arcsin\sqrt{\frac{I - I_{min}}{I_{max} - I_{min}}}\right) \tag{6}$$

where I_{max} and I_{min} denote the maximal and minimal intensity of the reflected light respectively, $k = 0, 1,...$ is the order of the interference maximum, λ is the wavelength of the incident light (546 nm in our case), and n_0 is the refractive index of the liquid forming the film. A photomultiplier tube (PMT) is employed to determine the intensity of the reflected light with great precision. Thus, the film thickness is calculated with maximal uncertainty of about 1 nm. When an effective water thickness is employed, one considers the film as *uniform*. It is possible to consider the stabilizing surfactant (protein) layers separately from the water core,[13] but this requires detailed information about the thickness and refractive indexes of these layers. Because the physical properties of the protein layers are strongly dependent on the sample history, the literature data for the thickness and refractive index of the protein layers are not always consistent. For this reason, we do not speculate about the structure of the film and always consider the effective water thickness.

Because we have the possibility to measure independently the disjoining pressure and the film thickness, we are able to evaluate disjoining pressure versus thickness isotherms, $\Pi(h)$. The method allows only the repulsive branch(es) of the disjoining pressure isotherm to be determined. The experimental results are described in the following sections.

2.2. Materials and Methods. *Hexadecane.* The hexadecane used as an oil phase in the TLF studies was of analytical grade. It was purchased from Merck and was used as received.

The Proteins. Bovine serum albumin, essentially fatty acid free (BSA), β-lactoglobulin (BLG), and β-casein were Sigma products (catalog numbers A-7511, L-0130, B-6905; lots 102H-93101, 91H7005, and 25H9550, respectively). Tween 20 was purchased from Fisher Scientific (ICI Surfactants, enzymatical grade, lot 982322). All surface-active products were used as received. The NaCl used for fixing the ionic strength was a Merck product. It was baked for approximately 5 h at 450 °C to remove any organic contamination. All solutions were prepared using water purified by a Milli-Q unit (Millipore), resistance 18.2 MΩ. cm^{-1}. The solutions were stored for no more than 20 h; hence, no bactericide was added. All experiments were carried out at room temperature of 22 ± 1 °C. The ability of proteins to buffer the pH of their solutions is well-known, and the pH established after dissolving a certain amount of protein in water is frequently referred to as "natural pH". In all cases, we worked at the natural pH of the proteins, which was 5.7 for BSA, 6.0 for BLG, and 6.1 for β-casein. This way of maintaining the pH was chosen because

(19) Said, A. S. *The Theory of Chromatography*; Dr. Alfred Hüthing Verlag: Heidelberg, Germany, 1981.

(20) Scheludko, A. *Annual Reports of the Sofia University, Faculty of Chemistry*; Sofia University: Sofia, Bulgaria, 1964−1965; Vol. 59, p 263.

Table 1. Comparison of the Calculated and Measured Disjoining Pressure for Small Films in the Present Experimental Configuration

film diameter (μm)	film type	surfactant	calcd pressure (Pa)	measured pressure (Pa)
190	foam	3 wt % BSA	118	$103 \pm 5\%$
230	foam	$100 \times$ cmc Tween 20	90	$95 \pm 6\%$
210	emulsion	1.5 wt % BSA	25	$21 \pm 10\%$

it makes it possible to work at low ionic strength (mostly 0.001 M NaCl). Any additional adjustment of the pH (either by conventional buffer or by adding a controlled amount of acid/base) increases the ionic strength. The pH of Tween 20 solutions was 5.4. All pH values were measured by means of a digital pH meter, equipped with a protein and surfactant resistant electrode. No drift of the pH values of the protein solutions was observed over the period of storage.

Glassware. All glassware (including the cells) was soaked for 20 min in concentrated chromic–sulfuric acid and then thoroughly rinsed with abundant quantities of Millipore-purified water and finally dried at 50 °C in a closed chamber.

Measurements of the Interfacial Tension. The measurements of the interfacial tension were performed on a Krüss tensiometer, using the du Nouy ring method. The measurements were performed on protein solutions of corresponding concentration and ionic strength of 0.001 M (maintained also with NaCl) at natural pH and at room temperature of 22 °C. The values were taken 19–20 h after loading the two liquid phases into the measuring vessel. According to the literature data,[21] this time is sufficient for reaching equilibrium between the bulk and the interface. In a parallel experiment, we checked that in each case a constant value of the interfacial tension is reached for even shorter times, say 12–14 h. The measured interfacial tension values were as follows: 14.5 mN/m for β-casein, 17.3 mN/m for BSA, 15.9 mN/m for BLG.

3. Results and Discussion

3.1. Reliability Tests of the Novel Version of the Mysels Cell. A few cells were used in the experiments. They differ in the size of the pores, i.e., in the maximum attainable capillary pressure. The cells, as well as the reproducibility of the method, were tested with foam and emulsion films, stabilized by the low-molecular-weight surfactant Tween 20 and by the globular protein BSA. For small films, it was possible to calculate the capillary pressure theoretically, according to eq 1, and to compare it with the measured values. Table 1 summarizes the results. As one can see, the agreement is quite good.

We would like to emphasize that our experimental setup cell gives the opportunity to measure in a well-controllable way the capillary (disjoining) pressure and the respective film thickness. Of course, to do this one should take all precautions to ensure the absence of possible artifacts (see the next section).

3.2. Possible Artifacts in the Case of Protein-Stabilized Films. *3.2.1. Hydrophobization.* It is well-known that the proteins tend to adsorb on all kinds of surfaces, thus modifying their properties. This is a major complication when studying protein-stabilized films. When a hydrophilic substrate (a glass surface, for example) is exposed to a protein solution, the adsorption of the protein on it generally leads to hydrophobization of the surface. The possibility of hydrophobization of the glass cell when in contact with protein solution should not be disregarded. This can influence substantially the stability of the film. Note that the perfect wetting of the cell walls by the liquid
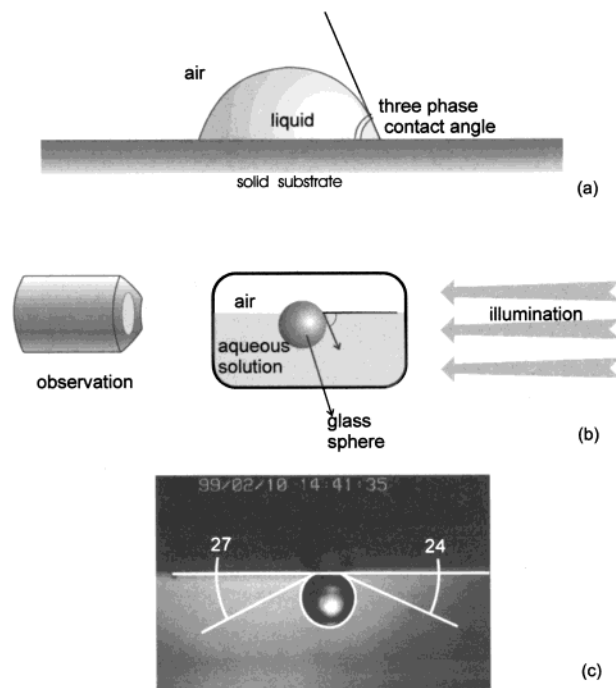
(21) Lucassen-Reynders, E.; Benjamins, J. In *Food Emulsions and Foams Interfaces, Interactions and Stability*; Dickinson, E., Rodríguez Patino, J. M., Eds.; Royal Society of Chemistry: Cambridge, U.K., 1999; p 195.
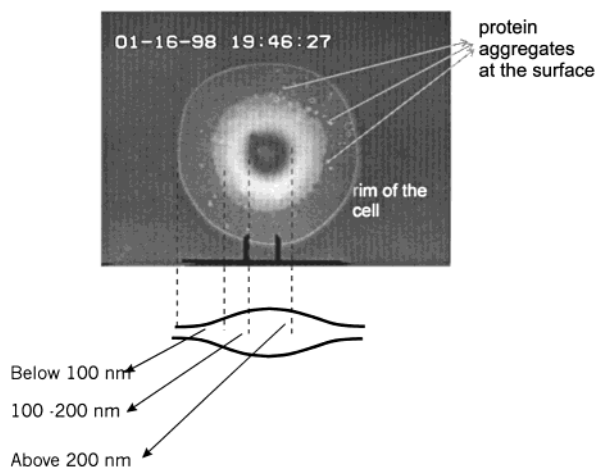

Figure 2. (a) Schematic of the three-phase contact angle, (b) scheme of the experimental setup, (c) photograph of a hydrophobized glass sphere attached at the air/water interface. The measured three-phase contact angle is also shown.

forming the film is a necessary prerequisite for stable films. When the cell is hydrophobic, i.e., not perfectly wetted by the protein solution, the formed film detaches from the holder and ruptures. During our experiments, we observed that the disjoining pressure at which the protein films rupture is not well-reproducible. Apart from fluctuations, this effect may be caused by partial hydrophobization of the cell. To check this hypothesis, we performed a model experiment to verify how the protein adsorption changes the hydrophilicity of a glass sphere. The degree of hydrophobization is well-characterized by the three-phase contact angle, formed between the gas (air), solid (glass), and liquid (protein solution) phases (see Figure 2). A convenient way to measure relatively large three-phase contact angles is to attach a small solid (glass) sphere at an air/liquid interface. When the contact angle is small (say 0°–10°), i.e., a hydrophilic sphere, the sphere cannot be fixed at the interface because the force balance cannot be satisfied. But a hydrophobic sphere of the same size and density is easily attached at the air/water interface because of the large contact angle. A perfectly hydrophilic glass sphere (cleaned exactly as the cells; with radius of 0.3–0.4 mm) was immersed in BSA solution for a period of 2 h. The protein concentration was varied from 0.02 wt % to 0.1 wt %. Then, the sphere was thoroughly dried at room temperature in a closed chamber to avoid any contamination. The treated sphere was gently placed at the air/protein solution interface. The system was observed in transmitted illumination (see Figure 2). The images were recorded by means of a video system and further processed with image analysis software. The three-phase contact angle was determined goniometrically. A typical picture is shown in Figure 2c. One can see that the contact angle is about 25°–28°, a value that was reproducible and essentially independent of the protein concentration. Note that when the sphere was not soaked in protein solution, it was entirely hydrophilic.

The experiment described above is important because it demonstrates a possible change of the surface properties

Figure 3. Photomicrograph of a BSA-stabilized film with adhered periphery. A vertical cross-section is schematically presented, and the approximate thickness is shown. The white spots are protein clusters at the film interface. The thickness of the film at these points is between 100 and 200 nm. The distance between the bars is 100 microns.

of the glass during experiments in which protein solutions are involved. It is worthwhile to point out that the period of contact of the model sphere with the protein solution is comparable with the time scale of the real experiments with emulsion/foam films. Hence, the "unexpected" rupture of relatively thick protein-stabilized films at low capillary pressure may result from the hydrophobization of the film holder. For this reason, in each case when protein-stabilized films were investigated, we performed a few experiments (each of them conducted employing a freshly cleaned cell). The disjoining pressure vs distance isotherms presented here are actually a superposition of several experiments (see below).

3.2.2. Periphery Sticking. Generally, the rapid formation of a large film is accompanied by creation of a dimple inside the film.[10] The appearance and the expelling (in a few seconds) of the dimple are due to the interplay between hydrodynamic and surface forces. When a protein-stabilized film is rapidly formed, the hydrodynamic dimple practically does not flow out even for hours. The periphery of the film thins down, and the two surfaces stick together. Thus, the sticking around the periphery prohibits the shape relaxation of the film. An example is presented in Figure 3. Because this phenomenon was observed only in the case of protein-stabilized films, one can conclude that the effect is somehow due to specific surface-rheology properties of the protein layers, as well as to cross-linking/aggregation of the species adsorbed at the two film surfaces. We noticed also that the effect is more pronounced at high ionic strengths, at which the electrostatic repulsion is suppressed. Because the thickness measurement implies plane-parallel film, one needs to choose such conditions of making films that the periphery sticking does not take place. In an attempt to avoid the periphery sticking, we manipulated the protein-stabilized films extremely gently and slowly and worked at low ionic strength. The data presented in the next sections are taken on plane-parallel films only.

3.2.3. Protein Aggregation. As already stated, the interferometric method for thickness determination is applicable only to perfectly plane-parallel films. When the protein is aggregated, the large clusters at the film surfaces make the evaluation of the film thickness impossible. In the case of BSA-stabilized thin liquid films,
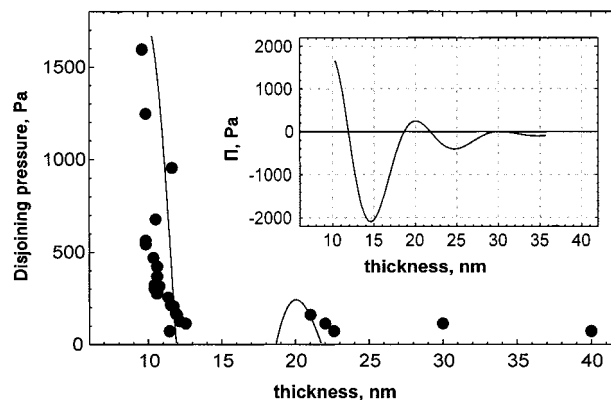

Figure 4. Disjoining pressure vs thickness isotherm of a foam film stabilized by Tween 20, 600 × cmc, 0.1 M NaCl (the points). The solid line is the best fit; see the text for details. The inset shows the fit only.

it is found[22] that the aggregate formation takes place at the surface because no clustering in the bulk protein solution was observed. We have a similar observation in the case of BLG-stabilized foam and emulsion films. Dynamic light scattering (DLS) experiments showed no visible aggregation in preliminary filtered (400 nm cutoff) bulk BLG solutions over a period of 2−3 days. The DLS measurements revealed objects of 3−4 nm in size, which corresponds to the size of the individual protein molecules. Furthermore, we noticed that only the first 1−2 films formed just after loading the cell are essentially free from aggregates, i.e., suitable for determination of the thickness. After a few films (say 3−4) have formed and ruptured, the aggregation becomes considerable (Figure 3). This leads to a high degree of roughness of the interfaces. In Figure 3, aggregates appear like bright spots, which implies that the local thickness there is above 100 nm. Any analysis concerning the origin of the phenomenon requires an interpretation at a molecular level, which is impossible to do without appropriate experimental data. Hence, we restrict ourselves to specifying that to measure correctly the film thickness, we always studied the first or the second film formed after loading the cell.

3.3. Tween 20. We investigated the disjoining pressure versus distance isotherm for a foam film, stabilized by the nonionic surfactant Tween 20. This is a very good model system because the properties of this surfactant have been extensively studied in recent years.[23] We work with foam films here to avoid the nonequilibrium effects connected with the surfactant redistribution between the oil and water phase.[15] In these experiments, we also checked the reproducibility of our technique. We worked at a concentration of 600 × cmc in the presence of 0.1 M NaCl. The disjoining pressure isotherm is shown in Figure 4. Three independent runs are plotted together in a common plot.

The high surfactant concentration gives rise to oscillatory structural forces. The film thins in a stepwise manner, i.e., stratification was observed. The line in Figure 4 is the best fit of our data supposing additivity of the oscillatory structural forces and the Derjaguin−Landau−Verwey−Overbeek (DLVO) forces (i.e., van der Waals attraction and electrostatic repulsion). In this case, the disjoining pressure is represented as

$$\Pi_{tot}(h) = \Pi_{osc}(h) + \Pi_{vW}(h) + \Pi_{el}(h) \tag{7}$$

The explicit expressions for the different components of

(22) Gurkov, T. D.; Marinova, K. G.; Zdravkov, A. Z.; Oleksiak, C.; Campbell, B. *Prog. Colloid Polym. Sci.* **1998**, *110*, 263.

the disjoining pressure are as follows: for van der Waals attraction,

$$\Pi_{vW} = -\frac{A_H}{6\pi h^3} \tag{8}$$

where A_H is the Hamaker constant. The electrostatic contribution to the total disjoining pressure is calculated through the expression

$$\Pi_{el}(h) = 64\,C_{el}kT\tanh^2\!\left(\frac{e\Psi_s}{4kT}\right)\exp(-\kappa h) \tag{9}$$

where C_{el} is the electrolyte number concentration, kT is the thermal energy, and κ is the inverse Debye length. Ψ_s and e denote the surface potential and the elementary charge, respectively. The oscillatory structural component of the disjoining pressure was calculated via a recently proposed semiempirical expression:[15]

$$\Pi_{osc}(h) = P_0 \cos\!\left(\frac{2\pi h}{d_1}\right)\exp\!\left(\frac{d^3}{d_1^{\,2}d_2} - \frac{h}{d_2}\right) \quad for \quad h > d$$

$$\Pi_{osc}(h) = -P_0 \quad for \quad 0 < h < d \tag{10}$$

where d is the diameter of the micelles and P_0 is the osmotic pressure exerted by the micelles. P_0 was calculated via the Carnahan–Starling formula:

$$P_0 = nkT\frac{1 + \phi + \phi^2 - \phi^3}{(1 - \phi)^3} \tag{11}$$

where n is the micellar number density and ϕ is the volume fraction of the micelles. In eq 10, d_1 and d_2 are the period and decay length of the oscillations, respectively. These two quantities are related to the micellar volume fraction as

$$\frac{d_1}{d} = \sqrt{\frac{2}{3}} + 0.237\Delta\phi + 0.633(\Delta\phi)^2;$$

$$\frac{d_2}{d} = \frac{0.4866}{\Delta\phi} - 0.420 \tag{12}$$

In the expressions in eq 12, $\Delta\phi = \phi_{max} - \phi$ with $\phi_{max} = \pi/(3\sqrt{2})$. The Debye atmosphere surrounding the micelles was also taken into account in the calculation of the volume fraction of the micelles. In our case, the ionic strength is high and the Debye length is 1 nm. Taking a Hamaker constant of 3.7×10^{-20} J, a micellar diameter of 7.4 nm,[24] and aggregation number of 80, one fits the data in Figure 4 using as a free parameter only the surface potential, Ψ_s. The value obtained from the fit is -20 mV, which is in reasonable correlation with the experimentally measured value for the ζ-potential (-23 ± 3 mV) of Tween 20-covered xylene droplets.[25,26] The final thickness of the film (10–12 nm) corresponds to one micellar layer entrapped between the film surfaces.[26]

3.4. β-casein. We measured the pressure vs thickness isotherms of emulsion films stabilized by 0.1 wt % β-casein. The ionic strength was maintained by 0.001 M NaCl, at natural pH of 6.1 ± 0.1. In this case, we found a purely DLVO behavior. Figure 5a shows the experimentally
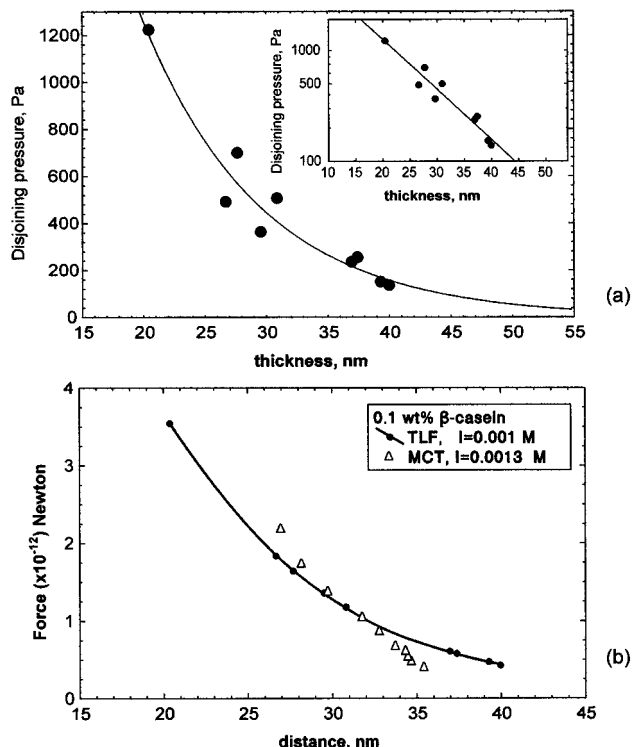

Figure 5. (a) Disjoining pressure vs thickness isotherm for an emulsion film stabilized with 0.1 wt % β-casein (points) and best DLVO-fit (line). The ionic strength is 0.001 M NaCl; pH = 6.1. The inset shows the same data in log plot. Panel b shows the comparison between the force calculated from the experimental data in panel a and the force measured by employing the MCT (refs 24, 25).

obtained $\Pi(h)$ isotherm (points), as well as the best DLVO fit (line). The fit is made supposing constant surface potential; the plane of charge was taken to coincide with the water/oil interface. The value of the Hamaker constant was 0.49×10^{-20} J. The only free parameter was the surface potential, which was found to be -27.8 mV. This value agrees fairly well with the data in the literature[25,27] (30–36 mV) for the ζ-potential of β-casein-covered particles. Because the stabilizing protein is reported in the literature to form micelle-like aggregates of various sizes, it was important to estimate the magnitude of the oscillatory structural forces, which can arise from the excluded volume effects. Taking the average diameter of the β-casein aggregates (micelles) to be 26 nm[28] and 250 kDa[29] for their molecular mass, one calculates exactly (eqs 10–12) the contribution of the oscillatory disjoining pressure to the measured pressure. The calculations showed that the volume fraction of the micelles is less than 2% and the oscillatory pressure exerted by them is of the order of magnitude of the experimental uncertainty in the pressure determination. The osmotic pressure exerted by the micelles is about 10 Pa. Therefore, we can stipulate that in the studied system the operative force is mainly the electrostatic repulsion (at distances larger than 20 nm, as here, the influence of the van der Waals interactions is minor). The final thickness of about 20 nm measured in our experiment corresponds to 2 times the thickness of a single β-casein interfacial layer, the thickness of which is reported to be about 10 nm.[30]

(23) Gurkov, T. D.; Horozov, T. S.; Ivanov, I. B.; Borwankar, R. P. *Colloids Surf.* **1994**, *87*, 81.
(24) Dimitrova, T. D.; Leal-Calderon, F. *Langmuir* **1999**, *15*, 8813.
(25) Dimitrova, T. Ph.D. Thesis, Universitè Bordeaux I, France, 2000.
(26) Velev, O. D.; Marinova, K. M.; Alargova, R. A.; Ivanov, I. B.; Borwankar, R. P. *Proceedings of the First Congress on Emulsion*; 1993.

(27) Velev, O. D.; Campbell, B. E.; Borwankar, R. P. *Langmuir* **1998**, *14*, 4122.
(28) Leclerc, E.; Calmettes, P. *Phys. Rev. Lett.* **1997**, *78*, 150.
(29) Dickinson, E.; Golding, M.; Povey, M. J. W. *J. Colloid Interface Sci.* **1997**, *185*, 515.
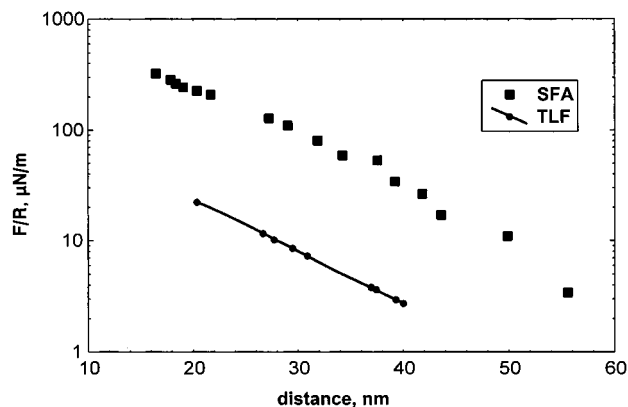
Figure 6. Comparison between the free energy per unit area calculated from the experimental data in Figure 5a and the free energy measured by employing the SFA (ref 32).

It is interesting to compare the results shown in Figure 5a with those obtained for very similar systems but employing the magnetic chaining technique[24,25] (MCT) and a surface force apparatus (SFA). Let us specify that MCT provides the force−distance laws existing between ca. 200 nm in diameter ferrofluid oil (octane + Fe_2O_3) droplets. By analytical integration over the thickness of the expression for the disjoining pressure (taking for the interfacial potential the value provided by the best fit), one obtains the corresponding force per unit length, $f(h)$, between two infinite planes:

$$f(h) = \int_h^\infty \Pi(h) \, dh \qquad (13)$$

Adopting the Derjaguin approximation,[31] one can find the real force, $F(h)$, acting between two spheres of equal radii, which is exactly the quantity measured in the MCT experiments:

$$F(h) = \pi a f(h) \qquad (14a)$$

where a is the radius of the spheres. In Figure 5b are compared the forces measured by means of the MCT (triangles) and the force calculated from the data in Figure 5a (line), as described above. Evidently, the two techniques lead to very similar results, which permits us to state that under these conditions the electrostatic repulsion is the main force governing the behavior of the studied system. The comparison plotted in Figure 5b demonstrates also that the two techniques explore approximately the same force range.

We transformed the data from Figure 5a in a similar way and obtained an expression for $F(h)/R$ (R being the radius of curvature of the mica sheets, typically about 1 cm) to compare with a typical SFA result.[32]

$$F(h)/R = 2\pi f(h) \qquad (14b)$$

The SFA data in ref 32 have been obtained for hydrophobized mica surfaces: protein concentration of 0.01 wt %, ionic strength of 0.001 M, and pH = 7. The superposition (Figure 6) of our data and the available literature data based on SFA experiments[32] demonstrates that the force laws are only qualitatively similar. This is more or less expected because the protein layers formed in the two

(30) Fang, Y.; Dalgleish, D. G. *J. Colloid Interface Sci.* **1993**, *156*, 329.
(31) Israelachvili, J. N. *Intermolecular and Surface Forces*; Academic Press: London, 1992.
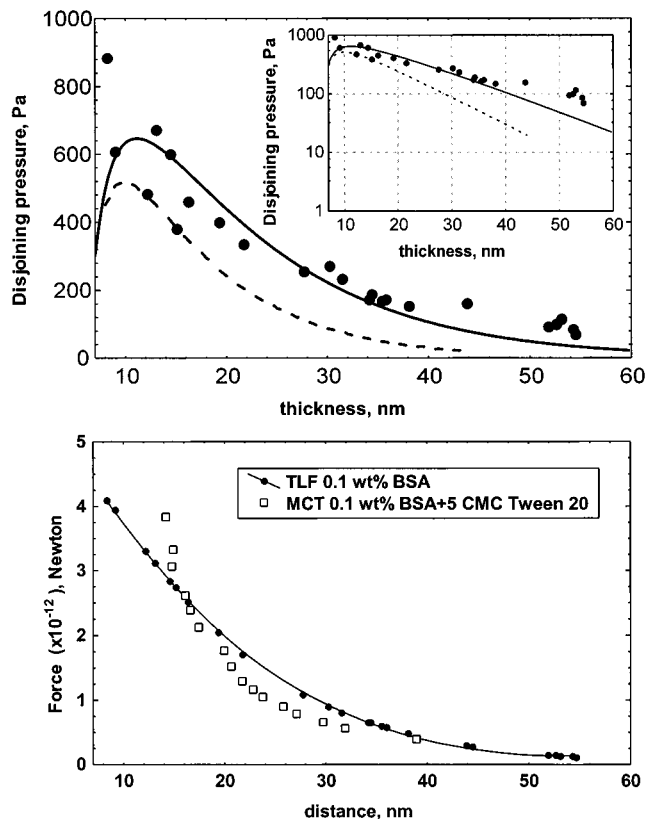(32) Nylander, T.; Wahlgren, M. N. *Langmuir* **1997**, *13*, 6219.

Figure 7. (a) Disjoining pressure vs distance isotherm for an emulsion film stabilized with 0.1 wt % BSA (points). The ionic strength is 0.001 M NaCl; pH = 5.7. The dashed line is the DLVO contribution; the solid line is the best fit assuming additivity of standard DLVO forces and steric-like repulsion (see text for details). The inset shows the same data in log plot. Panel b shows the comparison between the force calculated from the experimental data in panel a and the force measured by employing the MCT (refs 24, 25).

types of experiments are incompatible because of the differences in the conformation at the two types of surfaces. The difference between the values is about 1 decade; hence, no direct quantitative comparison is possible. We can therefore conclude that the data concerning the forces between protein layers formed at different interfaces should be handled with care.

3.5. BSA. We investigated also BSA-stabilized emulsion films, formed between hexadecane droplets. The concentration of the protein in the bulk aqueous phase was 0.1 wt %. The ionic strength, as in the previous cases, was fixed by 0.001 M NaCl, and the pH was 5.7 ± 0.1 (natural). The experimental results are shown in Figure 7a (points). The ζ-potentials of hexadecane droplets, covered by BSA, measured under similar pH and salt conditions[33] provided values between −5 and −10 mV. Hence, we used −10 mV for the surface potential to estimate the maximal DLVO contribution (dashed line in Figure 7a) to the total disjoining pressure. As in the case of β-casein, the Hamaker constant was 0.49×10^{-20} J and the Debye length was 9.6 nm (corresponding to 1 mM 1:1 electrolyte). Apparently, the measured repulsive pressure is longer-ranged compared to the one predicted by the DLVO model. It is established in the literature[34−36] that BSA layers exhibit

(33) van der Mei, H. C.; Meijer, S.; Busscher, H. J. *J. Colloid Interface Sci.* **1998**, *205*, 185.
(34) Fitzpatrick, H.; Luckham, P. F.; Eriksen, S.; Hammond, K. *Colloids Surf.* **1992**, *65*, 43.
(35) Gallinet, J. P.; Gauthier-Manuel, B. *Colloids Surf.* **1992**, *68*, 189.

strong and long-range steric repulsion, so it is natural to expect such interactions to be relevant in our case too. For numerous proteins, it is known[37,38] that after reaching the equilibrium interfacial tension (for a certain protein concentration) the adsorption, Γ, continues to increase. The latter fact is attributed to the formation of extra surface protein layer(s) of partially unfolded protein molecules (see, for example, ref 37). To take into account the formation of the second protein layer(s), one may use the approach of Israelachvili and Wennerström[39] and derive an expression for the disjoining pressure exerted by "ordering" of BSA entities just under the dense interfacial protein layer. Supposing the density, $\rho(z)$, of the second layer decreases exponentially with the distance, z, from the interface, we can write

$$\rho(z) = \rho(z_0) \exp(-h/\lambda^*) \quad (15)$$

where λ^* is the characteristic size of the protein species that constitutes the second layer. Let us neglect the correlations between the moieties in the subsurface layer and consider the case when two surfaces approach each other. Imposing nonoverlapping of the protein sublayers, one obtains the following expression for the repulsive pressure:[39]

$$\Pi_{\text{repulsion}}(h) = \frac{\Gamma_2(kT/\lambda^*)(h/\lambda^*)\exp(-h/\lambda^*)}{1 - (1 + h/\lambda^*)\exp(-h/\lambda^*)} \quad (16)$$

where Γ_2 is the adsorption in the second (subsurface) protein layer only. For distances larger than the characteristic size of the protein species forming the sublayer, eq 16 reduces to

$$\Pi_{\text{repulsion}}(h) = \Gamma_2(kT/\lambda^*)(h/\lambda^*)\exp(-h/\lambda^*) \quad (17)$$

Assuming additivity of the DLVO pressure and the repulsive steric pressure (eq 17), we fitted our experimental data using as free parameters Γ_2 and λ^* (solid line in Figure 7a). The values obtained were 0.23 mg/m² and 10.65 nm, respectively. From a physical point of view, these values are quite reasonable. An increase of the total adsorption (after the equilibrium value of the surface tension is reached) of about 0.5 mg/m² is reported in the literature.[40] This is exactly what Γ_2 stands for in our model. The value of λ^* is consistent with the size of the BSA molecule[41] (11.4 nm × 11.4 nm × 4.1 nm), as well as with the radius of gyration of a BSA molecule of ∼9 nm.

Let us now compare the data obtained employing the Mysels cell and the MCT. The experiments with ferrofluid-in-water emulsions, stabilized by mixtures of BSA and Tween 20, showed that the interactions between the droplets are to a large extent dominated by the quantity of BSA. That is why we compared the results for the disjoining pressure of emulsion films stabilized by 0.1 wt % BSA and those for ferrofluid particles stabilized by 0.1 wt % BSA + 5cmc Tween 20. The disjoining pressure is transformed into force in the same manner as in the case
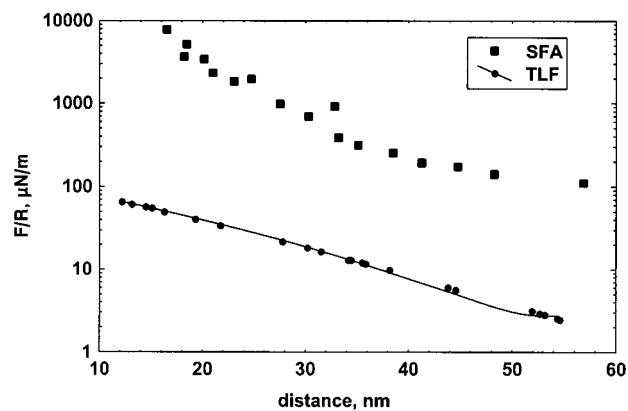
(36) Narsimhan, G. *Colloids Surf.* **1992**, *62*, 41.
(37) Graham, D. E.; Phillips, M. C. *J. Colloid Interface Sci.* **1979**, *70*, 403, 415, 427.
(38) Makievski, A. V.; Miller, R.; Fainerman, V. B.; Krägel, J.; Wüstneck, R. In *Food Emulsions and Foams Interfaces, Interactions, Stability*; Dickinson, E., Rodríguez Patino, J. M., Eds.; Royal Society of Chemistry: Cambridge, U.K., 1999; p 223.
(39) Israelachvili, J. N.; Wennerström, H. *J. Phys. Chem.* **1992**, *96*, 520.
(40) Lu, J. R.; Su, T. J.; Thomas, R. K. *J. Colloid Interface Sci.* **1999**, *213*, 426.
(41) Claesson, P. M.; Blomberg, E.; Fröberg, J. C.; Nylander, T.; Arnebrant, T. *Adv. Colloid Interface Sci.* **1995**, *57*, 161.

Figure 8. Comparison between the free energy per unit area calculated from the experimental data in Figure 7a and the free energy measured by the SFA (ref 34).
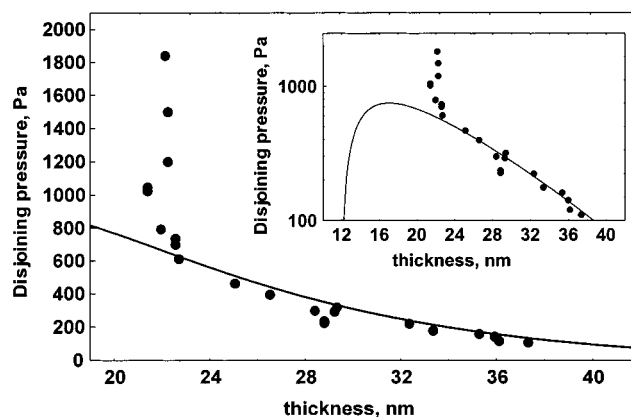

Figure 9. Disjoining pressure vs thickness isotherm of a foam film stabilized by 0.2 wt % BLG, 0.001 M NaCl, and natural pH (points). The solid line is the best DLVO fit. The inset shows the same data in log-plot.

of β-casein. The two force laws are plotted together in Figure 7b and exhibit reasonable agreement, having in mind the differences in the experimental conditions. Again, the comparison between our data and the data provided by the SFA[34] (data taken for BSA adsorbed on hydrophobic mica, bulk protein content of 5 × 10⁻⁴ wt %, pH = 5.5, ionic strength of 2 × 10⁻⁴ M) reveals only qualitative agreement, the reason being essentially the same as in the case of β-casein-stabilized films (Figure 8).

3.6. BLG. We performed experiments on foam films stabilized by 0.2 wt % BLG. Figure 9 summarizes the results. The points represent a common plot of three independent experiments. The ionic strength was fixed by adding 0.001 M NaCl. The pH was the natural one, 6.0 ± 0.1. The observed disjoining pressure profile is of DLVO-type for distances between 40 and 22 nm. We fitted the experimental points for the disjoining pressure by a conventional DLVO isotherm (eqs 7−9), varying as free parameter only the surface potential. The steep part of the dependence $\Pi(h)$ was not considered. The line in Figure 9 is the best fit. From the fit, we obtained a surface potential of 28.4 mV. As seen from the plot, at a separation of about 22−23 nm, the profile deviates from the electrostatic repulsion indicating the presence of relatively long-range specific protein−protein interactions. We believe that this steric-like repulsion is a manifestation of an overlap of extended protein layers. Experiments employing neutron reflectivity[42] have shown that the total

(42) Atkinson, P. J.; Dickinson, E.; Horne, D. S.; Richardson, R. M. *J. Chem. Soc., Faraday Trans.* **1995**, *91*, 2847.

thickness of a BLG adsorption layer at the air/water interface is 3−4 nm at a bulk protein concentration of 0.1 wt %. In those experiments, the adsorbed layer was assumed of uniform thickness and refractive index. At the same time, our own experiments with the MCT[25] showed that (i) BLG-stabilized droplets of radii 90 nm exhibit a steric-like repulsion at a surface to surface distance of 16 nm and (ii) the droplets irreversibly flocculate when pressed against each other by a force larger than 1.5×10^{-12} N. These two effects can be attributed to overlap of the protein layers on the approaching droplets, a process that makes some non-DLVO surface forces operative. Note that in absence of non-DLVO contributions the interfacial potential is high enough to prevent aggregation at such distance. We believe the same effect explains the steric branch of the disjoining pressure− distance isotherm taken on foam films (Figure 9). It is interesting to note that for both globular proteins (BSA and BLG) the steric-like interaction comes into play but it is not pronounced in the same way. The globular proteins are gradually unfolded when adsorbed at a liquid interface; hence, the intermolecular binding, cross-linking or both is facilitated. The exact structure of the BLG (and BSA) adsorption layer has not been completely clarified yet, and we are unable to provide a hypothesis concerning the type of the overlapping entities. Maybe there are small protein lumps, comprising dozens of BLG molecules.

4. Conclusions

A variant of the Mysels-type cell was developed and applied for modeling of food-type systems. It was found that the interaction between film interfaces covered by a simple surfactant (Tween 20) is very well-described theoretically assuming additivity of the DLVO forces and the oscillatory structural force. In the case of protein-stabilized films, the possible sources of artifacts and errors in the determination of the thickness and the disjoining pressure were examined and analyzed. Disjoining pressure vs distance isotherms were obtained for foam films stabilized by 0.2 wt % BLG and for emulsion films stabilized by 0.1 wt % β-casein and 0.1 wt % BSA. In all cases, the ionic strength was 0.001 M NaCl at natural pH. It was found that the interaction between the BLG layers is of DLVO-type at large distances, while at short distances an overlap of adsorbed protein entities takes place and the interaction turns into a steric-like steep repulsion. The interactions between β-casein layers formed at the water/hexadecane interface are governed by electrostatic repulsion. Because of the expanded protein layers at the interface, the film remains relatively thick, and the final thickness is about 20 nm. The van der Waals as well as the oscillatory component of the total disjoining pressure is found to be inferior in the case of β-casein. For BSA-stabilized films, a long-range repulsion is operative. It is not of an electrostatic origin, as both experiment and calculations proved. It most probably originates from the formation of multiple protein layers at the interface, an effect that is well-documented in the literature. A fit of the disjoining pressure vs thickness measured in this case is obtained assuming additivity of the classical DLVO disjoining pressure and a steric-like repulsive pressure brought by the formation of protein multilayers at the interfaces.

The disjoining pressure measured in the case of emulsion films was converted to force, adopting the Derjaguin approximation, and was compared with the direct force measurements performed employing the MCT. In all cases a reasonable agreement is observed. Let us emphasize that when protein-stabilized films were investigated, we always took all necessary precautions to ensure no surface aggregation (part 3.2). All possibilities for a rapid distortion of the protein-covered interfaces were strictly avoided. In other words, the films were formed and investigated in quasi-stationary conditions. When the films are not manipulated gently, they always contain surface aggregates, which modify the properties of the interacting layers.

The experimental configuration described in the present work opens the way to study the behavior of emulsion films in conditions close to those in actual emulsion systems.

LA0111147